

Enhancement of Resolution of Ultrasound Images through REC and SAFT

Hans Bethe, Senior in EE, Bradley University

Abstract— One consuming aim in ultrasonic imaging is to improve the axial and lateral resolutions of ultrasonic images. Axial and lateral resolutions are determined by transducer bandwidth and beamformation process. This project strives to investigate and simulate novel methods for exciting a linear array transducer and a beamformation method that could improve the spatial resolution and signal-to-noise ratio (SNR) of an ultrasound image. To improve the axial resolution, resolution enhancement compression (REC) was employed to artificially increase the transducers bandwidth by exciting it with a pre-enhanced chirp. Improvements in lateral resolution was achieved by using synthetic transmit aperture (STA), a delay-and-sum beamformation method that used one transducer element at a time during transmission and uses all elements during reception. It is hypothesized that by combining REC and STA, both axial and lateral resolution could be improved simultaneously. REC and STA techniques were simulated with a 128-element linear array transducer using Field II and MATLAB. The resolution improvement derived from REC and STA were measured through two image quality metrics: modulation transfer function (MTF) and SNR. Simulations results demonstrated that, from the MTF, REC had an axial resolution 1.5 times better than conventional pulsing excitation method. Simulation results for STA yielded a substantial reduction in the amount of energy spreading which degrades resolution of images. Overall, simulation results confirmed the hypothesis that combining REC and STA could achieve simultaneous improvement in lateral and axial resolutions. This work has the potential to improve target detectability which could allow for earlier detection of tumors.)

I. INTRODUCTION

Ultrasonic imaging (UI) is very important in medical research, enabling doctors to visually examine various internal organs, cancer tumors inside the patients. One consuming aim in UI is to improve the spatial resolution (divided into 2 types: axial and lateral) and signal-to-noise (SNR) ratio of ultrasound images.

Research in UI discovered two novel methods that have the potential to improve the lateral resolution and SNR of ultrasound images. One method is termed resolution enhancement compression (REC) which is capable of improving the axial resolution and SNR. The other method is termed synthetic transmit aperture (STA) that is capable of improving the lateral resolution and SNR through delay-and-sum processing.

The aim of this project was to conduct an investigation to acquire theoretical knowledge of REC and STA, then perform simulation of REC and STA based on the knowledge to

determine if the combined application of the two techniques can improve the spatial resolution and SNR of ultrasound images. The simulation was implemented through Field II software package.

II. THEORY

A. REC

The axial resolution of ultrasound images is influenced by the bandwidth of the transducer. The larger (narrower) is the bandwidth, the higher (lower) is the axial resolution. Prior to the discovery of REC, the method employed in UI was conventional pulsing (CP). CP excited the transducer by an electrical impulse. One serious drawback inherent in CP was that it could not yield high axial resolution if the bandwidth of the transducer was narrower.

REC can improve the axial resolution even with a spectrally narrow transducer. One of the central aspects of REC is the generation of an excitation signal referred to as pre-enhanced chirp. This chirp can artificially enlarge the bandwidth of the transducer, thereby yielding higher axial resolution. The enabling theory from which REC is derived is the convolution equivalence principle, whose mathematical characterization is shown below [1]:

$$h_1(t) * V_{pre-chirp}(t) = h_2(t) * V_{lin-chirp}(t) \quad (1)$$

The physical significance of equation (1) is: if the actual transducer characterized by impulse response $h_1(t)$ is excited by the pre-enhanced chirp (denoted $V_{pre-chirp}(t)$), then the ultrasonic pulse generated by this actual transducer will be almost identical to that generated by a transducer having a larger bandwidth characterized by impulse response $h_2(t)$ when it is excited by a simple linear chirp (denoted $V_{lin-chirp}(t)$) [1]. This theory suggests that by exciting the transducer having a narrower bandwidth with the pre-enhanced chirp, this transducer can yield the same axial resolution as can the transducer with a larger bandwidth when it is excited by a simple linear chirp, thereby translating into a higher axial resolution.

The transducer will be excited by the pre-enhanced chirp to generate the ultrasonic pulse that will travel and reach a target. The echoes reflecting back from that target will be compressed by a Wiener pulse compression filter, described by the following equation:

$$\beta(f) = \frac{V_{lin-chirp}^*(f)}{|V_{lin-chirp}(f)| + \gamma sSNR}^{-1} \quad (2)$$

Here:

1. $V_{lin-chirp}^*(f)$: is the frequency spectrum of a modified linear chirp. Note that this chirp is not the linear chirp shown in equation (1). This is because after the pre-enhanced chirp is generated based on equation (1), it is tapered by a Hanning window. Convolution equivalence principle thus no longer holds. If the original linear chirp is used in the Wiener compression filter (2), then considerable side lobes will emerge [1]. The equation used to derive the modified linear chirp is shown below [2]:

$$V_{lin-chirp}'(f) = \frac{H_2^*(f)}{|H_2(f)|^2 + |H_2(f)|^{-2}} H_{out}(f) \quad (3)$$

Where $H_{out}(f)$ is the frequency spectrum of the ultrasound pulse produced by the transducer after being excited by a pre-enhanced chirp.

2. γ : a parameter whose value range is [0; 1]. It varies the operating point of the filter (4) between the inverse and matched filtering. Smaller values of the gamma makes the filter approach an inverse filter, which yields higher axial resolution at the expense of SNR. Higher values of gamma makes the filter approach a matched filter, which improves SNR at the expense of axial resolution [1].

The metrics employed to assess the quality of REC are: SNR and modulation transfer function (MTF). The MTF is used to measure the axial resolution of an imaging system. From a plot of the MTF, one parameter can be extracted and used to determine the axial resolution, the wave number $k_0(m^{-1})$, which is used in the following equation:

$$\lambda = \frac{1}{2} \frac{2\pi}{k_0} (m) \quad (4)$$

The magnitude of lambda provides a measure of the axial resolution. The larger (smaller) lambda is, the higher (lower) the axial resolution. Because λ is a constant, the only way to decrease λ is to make k_0 larger.

A. STA

STA is one of the four beam-forming techniques collectively referred to as synthetic aperture focusing techniques (SAFT). Assumed a linear array transducer, for each emission, only one element in the transducer is active, and for each reception, all elements will be active. This pattern is repeated until all elements in the transducer have emitted. Each emission and reception generates one low resolution image (LRI). The number of LRIs corresponds to the number of elements in the linear array transducer. After all LRIs have been generated, they will be summed together to create a high resolution image (HRI)[3].

Due to delaying process, the LRIs corresponding to different elements in the transducer will appear to be out of phase. If this out-of-phase phenomenon is not resolved, then the HRI generated by summing all of the LRIs will exhibit significant energy spreading in the region around the point

target, which will in turn degrade the lateral resolution and SNR. STA remedies the out-of-phase problem by implementing delay processing for the LRIs before summing them to yield the HRI.

The metrics used to assess the quality of STA are similar to those used for REC: SNR and MTF.

III. Methods and Results

A. REC

There were two primary objectives in the simulation of REC. The first was to generate the pre-enhanced chirp used to excite the transducer. The second was to compress the echoes.

The first objective could be illustrated with figure 1 shown below:

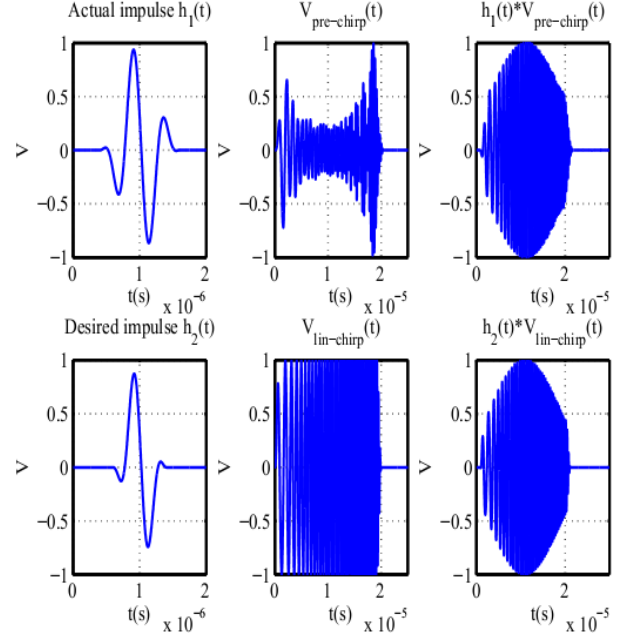


Fig. 1: Starting from upper leftmost figure and in clockwise direction: impulse response $h_1(t)$ of the actual transducer, pre-enhanced chirp, ultrasonic pulse produced by exciting $h_1(t)$ with pre-enhanced chirp, linear chirp, impulse response $h_2(t)$ of the transducer whose bandwidth is 1.5 times larger than that of $h_1(t)$

The process of generating the pre-enhanced chirp began with creating the waveform $h_1(t)$ which simulated the impulse response of the actual transducer. A Hanning window was then applied to $h_1(t)$ to create $h_2(t)$, which was narrower than $h_1(t)$ in terms of temporal duration. Then the linear chirp (designated as $V_{lin-chirp}(t)$ on figure (1)) was generated. The pre-enhanced chirp (designated as $V_{pre-chirp}(t)$ on figure (1)) could be generated by invoking the convolution equivalence principle:

$$h_1(t) * V_{pre-chirp}(t) = h_2(t) * V_{lin-chirp}(t) \quad (1)$$

$$\Leftrightarrow H_1(f) V_{pre-chirp}(f) = H_2(f) V_{lin-chirp}(f)$$

$$\Leftrightarrow V_{pre-chirp}(f) = \frac{H_2(f)}{H_1(f)} V_{lin-chirp}(f)$$

But there was a catch inherent in equation (6). If $H_1(f)$ is small, then simply dividing by $H_1(f)$ could magnify the noise. Therefore, in the simulation, the following equation was used to generate the pre-enhanced chirp [4]:

$$V_{pre-chirp}(f) = \frac{H_2(f)H_1^*(f)}{|H_1(f)|^2 + |H_1(f)|^{-2}} V_{lin-chirp}(f) \quad (7)$$

By implementing equation (7) in MATLAB, the pre-enhanced chirp and the ultrasound pulse generated by the transducer $h_1(t)$ in figure (1) were shown in figure (2) below:

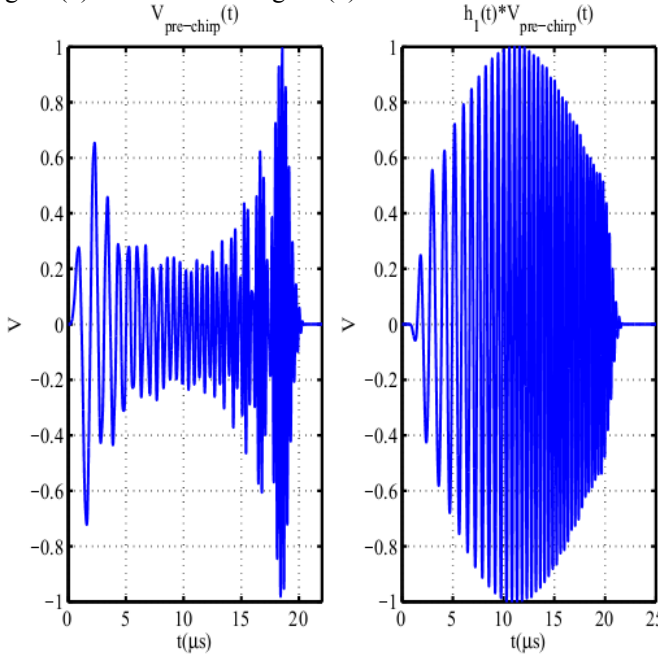


Fig. 2: Left: pre-enhanced chirp. Right: the ultrasound pulse generated by excitation of transducer $h(t)$ with pre-enhanced chirp

The second objective was to compress the echo. To accomplish this, the echo had to be generated. This was done by distorting the ultrasound pulse shown in figure (2) with some random noise. Then the noise-corrupted echo would undergo pulse compression, whose mathematical representation was equation (2). The result of the pulse compression was shown in figure (3).

The middle figure of figure (3) showed the echo of REC after undergoing compression by the Wiener pulse compression filter (2). Compared to the uncompressed echo of CP, the compressed echo of REC exhibited less noise and thus improved the SNR of the image.

Note that the right figure showed that the main lobe in the envelope of REC was much narrower than that of CP. This meant that the axial resolution yielded by REC was higher than that yielded by CP.

From MATLAB computation, the SNR of REC was 46.37, of CP was 38.33 dB. This result confirmed the potential to improve the SNR brought allowed for by pulse compression of REC.

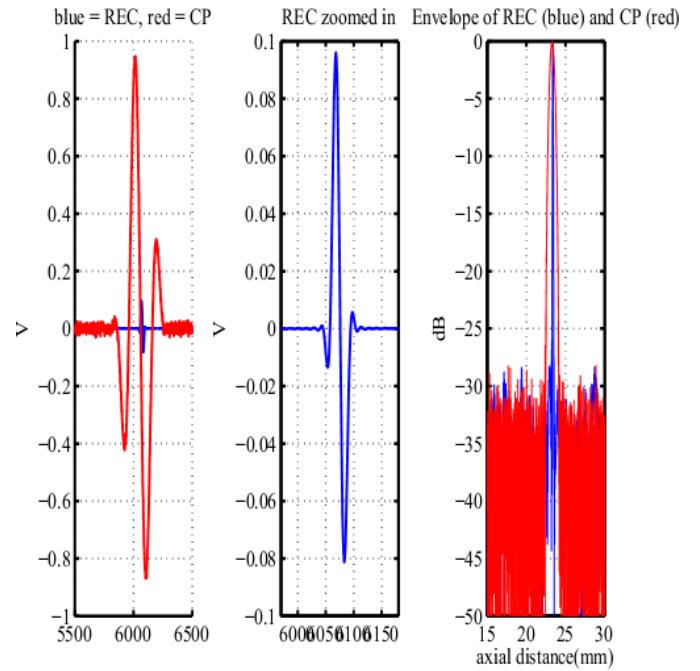


Fig. 3: Left: Comparison between the compressed echo of REC and the echo of conventional pulsing (CP). Middle: the zoomed-in image of the compressed echo of REC to demonstrate the reduction in noise. Right: the envelopes of the echo of CP and compressed echo of REC

The axial resolution of REC and CP was determined from the MTF curve shown in figure (4).

From the curve, the values of the k_0 corresponding to REC and CP were determined to be: 8342 and 5678, respectively. Using equation (4) and the knowledge that the larger the k_0 value is, the smaller λ becomes, which implies higher axial resolution. Since k_0 of REC was larger than that of CP, the axial resolution associated with REC was higher than that of CP. The improvement factor was $8342/5678 = 1.46$, suggesting that the axial resolution achieved by REC was about 1.5 times higher than that of CP. One noteworthy point: the improvement factor in axial resolution corresponded closely to the bandwidth expansion factor between the bandwidth of transducers $h_1(t)$ and $h_2(t)$ shown in figure (1). Since the 6-dB bandwidths of $h_1(t)$ and $h_2(t)$ were about 83% and 126%, respectively, the bandwidth expansion factor was about $(126/83 = 1.52)$. This value was fairly close to the axial resolution improvement factor of 1.46 derived above.

The improvement both in terms of axial resolution and SNR allowed for by REC demonstrated its superior performance over CP when both were used to excite the transducer.

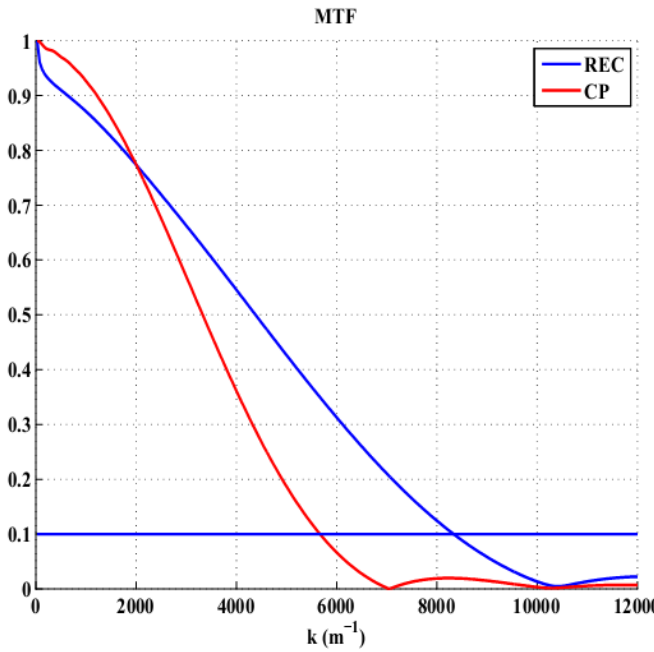


Fig. 4: Comparison between MTF curves of REC and CP

B. STA

The simulation of STA was performed through the Field II software package developed by the Technical University of Denmark. Field II was designed specifically for imaging application. It featured many special functions written to simulate different types of transducer, delaying, apodization and beam-forming. The first task in the simulation of STA was to create a linear array transducer based on the following specifications:

- 1) kerf (the distance between two contiguous elements): 40 μm
- 2) width of an element: 200 μm
- 3) height of an element: 5 mm
- 4) number of elements in the array: 128
- 5) fixed focus for the array (x,y,z): (0,0,40 mm)

The function in Field II that was invoked to create the linear array transducer with the aforementioned specifications was [5]:

$Th = xdc_linear_array(no_elements, width, \dots, height, kerf, no_sub_x; no_sub_y, focus)$

Where Th was a pointer pointing to the transducer. There were two additional input parameters in the above function: - no_sub_x and no_sub_y : the number of sub-elements in the x and y direction of the array. no_sub_x and no_sub_y were specified to be 2, 3, respectively, based on the example illustrating how a linear array transducer was created in Field II.

The step following the transducer creation was to excite the transducer with an impulse. This was accomplished using the following function in Field II [5]: $xdc_excitation(Th, pulse)$

where pulse was the impulse. The next step was to simulate the STA beam-forming technique. This was accomplished by invoking the following function in Field II [5]:

$calc_scat_all(emit_trans, rec_trans, positions, scat_amp, l)$

Where:

- 1) $emit_trans$ and rec_trans were the transducer apertures used in emitting the ultrasound pulses and receiving the echoes, respectively. In this simulation, both the emitting and receiving apertures were identical.
- 2) $positions$ was a matrix composed of 3 columns. The 1st, 2nd, and 3rd columns contained the values of the x,y,z coordinates of the point-like targets. In this simulation, the x and y coordinates were all set to be 0, while the z coordinates were set to be 30, 40, and 50 mm, respectively.
- 3) $scat_amp$: was a vector containing the values of the magnitude of the point-like targets in the simulation. For the sake of simplicity, the magnitude values were set to 1.

The above function generated a huge matrix storing the values of the echoes. The number of columns in this matrix equated to the product between the number of elements in the receiving and emitting apertures. Because the number of elements in both emitting and receiving apertures were 128 elements, the number of columns was thus $128 \times 128 = 16384$ columns. Furthermore, the matrix contained 128 sets of echoes, with each set being comprised of 128 echoes. Each of those set effectively represented one LRI corresponding to a particular transducer element. For example, the 1st echo set corresponded to the 1st element in the transducer, the 64th echo set corresponded to the 64th element in the transducer, and so on.

The aforementioned mechanism of the function $calc_scat_all$ could thus simulate the way STA emitted ultrasound pulses and received the echoes.

To illustrate the out-of-phase phenomenon mentioned in the theory of STA, referred to figure (5).

Quick examination of the LRIs shown in figure (5) demonstrated the out-of-phase phenomenon, which was reflected through the LRIs not being aligned with each other. The 64th appeared to return to the transducer the earliest, where as the 128th LRI returned to the transducer the latest. If this out-of-phase phenomenon was not eliminated by delay processing, then summing all of these out-of-phase LRIs would result in a HRI shown in figure (6).

The HRI in figure (6) exhibited a considerable amount of energy spreading around the region occupied by the point-like targets. This considerable loss of energy would degrade the SNR and also the spatial resolution of the image. To mitigate this problem, delay processing was implemented.

This delay processing consisted of the following steps:

- 1) Determined the echo set (which was an LRI) that returned to the transducer the earliest.
- 2) Determined the echo in the earliest echo set that returned to the transducer the earliest. Extracted the

index associated with the first non-zero value in the array containing the values of this echo.

- 3) Repeated step 2 for other echo sets. Extracted the indices corresponding to the first non-zero value in the array containing the values of the earliest echo in those echo sets.
- 4) Calculated the difference between the index determined in step 2 with those in step 3.
- 5) Shifted the echo sets that were not the earliest one by the amount that was equal to the differences determined in step 4.

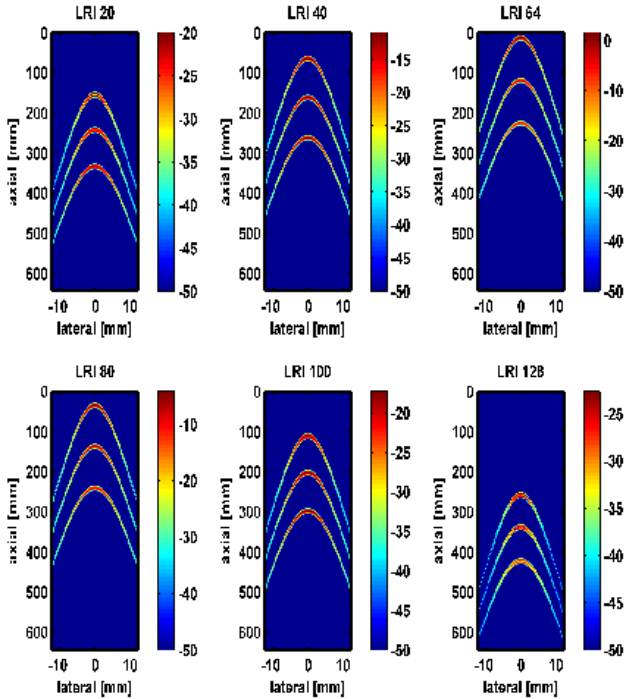


Fig. 5: Starting from top left figure and moving clockwise: the LRIs corresponding to the 20th, 40th, 80th, 100th, 128th elements of the linear array transducer.

The result of delay processing could be seen through the right plot in figure (7). It was clear that delay processing significantly reduced the amount of energy spreading around the region occupied by the point-like targets, which would in turn boosted the SNR.

MATLAB computation yielded the SNR before and after delay processing to be 36.89 dB and 50.44 dB, respectively.

Figure (8) displayed the MTF curves corresponding to STA before and after delay processing.

Measurements on the MTF curves in figure (8) yielded the following k_0 values: 407.3 m^{-1} and 454.1 m^{-1} corresponding to STA before and after delay processing, respectively. This meant that the delay processing yielded an improvement of $(454.1/407.3 = 1.11)$.

The simulation results thus demonstrated that STA's delay-and-sum processing could significantly improve the SNR and the axial resolution of the image.

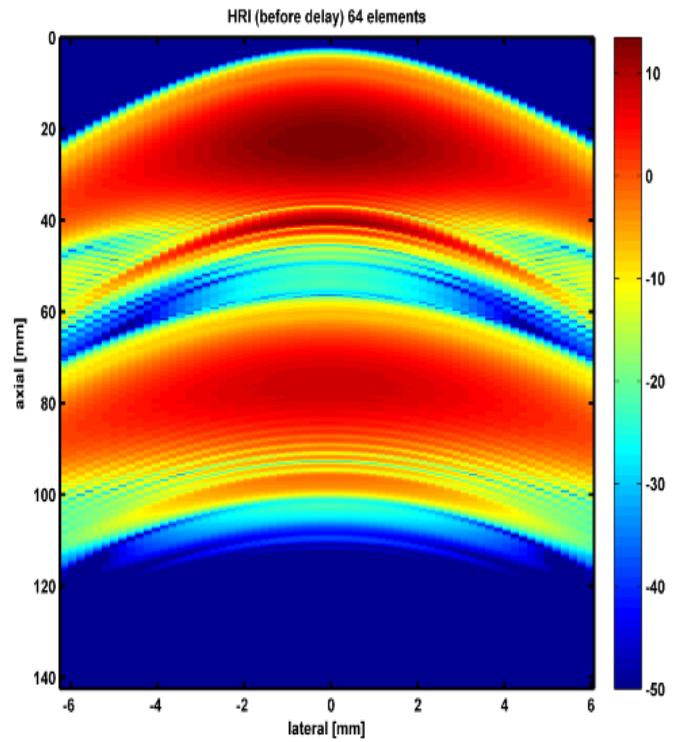


Fig 6: The HRI before delay processing, showing considerable amount of energy spreading around the region occupied by the point-like targets

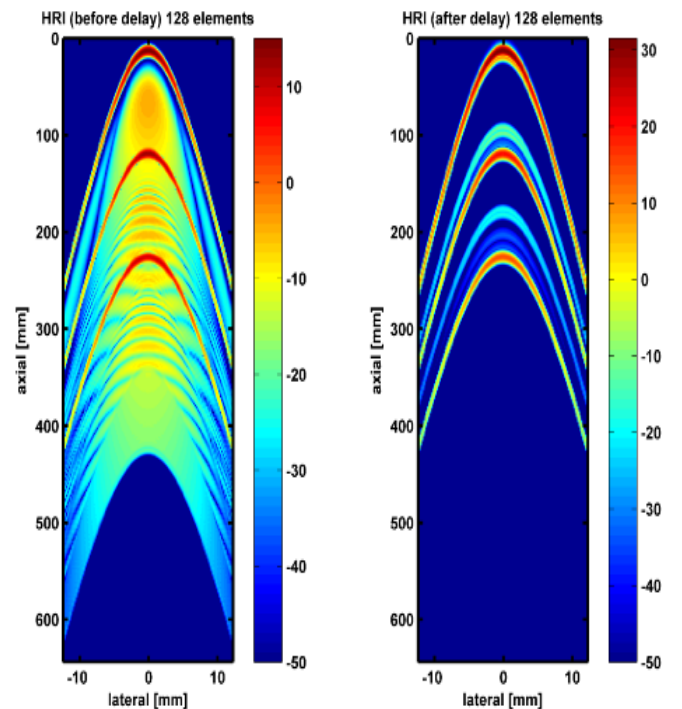


Fig 7: Comparison of HRI before and after delay processing was implemented

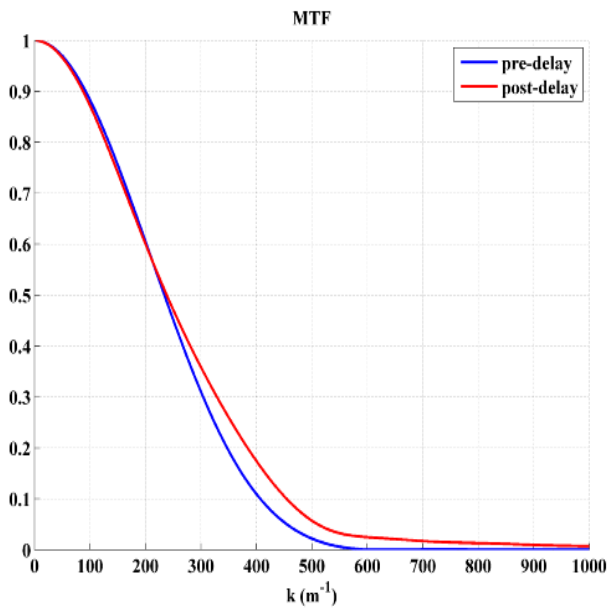


Fig 8: MTF curves of STA before and after delay processing.

The last step in the project was to combine REC and STA together to determine if the combined effect of REC and STA could yield an improvement in both axial and lateral resolution and the SNR of ultrasound images. This attempt to combine REC and STA did not succeed due to memory issue. Specifically, the amount of data to be processed was enormous which consumed a tremendous amount of memory storage that exceeded that allocated to the program.

IV. Conclusion

The project was truly challenging due to the advanced nature of the knowledge involved in the investigation. Specifically, the material on beam-forming required a great

level of knowledge in wave physics and advanced mathematics, which could prove very challenging to an investigator who was not well-versed in those field.

The project was quite frustrating because the programming endeavor often did not generate the expected or desired result. This experience was common during the simulation for REC, in which the generation of the pre-enhanced chirp was very time-consuming and involved a lot of trial and error to achieve the acceptable result. Another frustrating feature of the project was the difficulty visualizing how the ultrasound beam was formed and directed toward the targets. Because it

Despite all of the challenge and frustration, a significant amount of understanding and knowledge were acquired, especially in term of theory and programming experience. Specifically, the author understood how REC could help improve the axial resolution and the SNR, how the quality of REC could be measured by standard quality metrics. The author also learned about different beam-forming techniques and various aspects associated with them. Lastly, the author acquired a familiarity with Field II software program and also honed programming skills.

V. REFERENCES

- [1] M. Oelze, "Bandwidth and Resolution Enhancement through Pulse Com-pression", IEEE Transaction on Ultrasonics, Ferroelectric, and Frequency Control, vol. 54, no. 4, pp. 768-781, Apr. 2007
- [2] J. Sanchez, "Improving Ultrasonic Imaging using Novel Coded Excitation Techniques"
- [3] S. I. Nikolov, "Synthetic Aperture Tissue and Flow Ultrasound Imaging"
- [4] W. Ridgway, "Deep Structure Ultrasound Imaging Using Fundamental and Third Harmonic Coded Excitation Techniques"
- [5] J. A. Jensen, "Users' Guide for the Field II Program"